

## Inverse Kinematic Analysis of a 5 DOF Gantry Type Welding Robot

Nülfifer GÜNDOĞAN<sup>1\*</sup> , Cengiz DOĞAN<sup>2</sup> 

<sup>1</sup> Adıyaman Üniversitesi, Besni Ali Erdemoğlu MYO Vocational School, Electronics and Automation Department, Adıyaman, Türkiye

<sup>2</sup> Harran University, Engineering Faculty, Mechanical Engineering Department, Şanlıurfa, Türkiye  
Nülfifer GÜNDOĞAN ORCID No: 0000-0002-9464-0855  
Cengiz DOĞAN ORCID No: 0000-0002-1468-8462

\*Nülfifer GÜNDOĞAN: [ngundogan@adiyaman.edu.tr](mailto:ngundogan@adiyaman.edu.tr)

(Received: 05.02.2025, Accepted: 08.05.2025, Online Publication: 27.06.2025)

### Keywords

Homogeneous transformation matrix, Kinematic diagram, Inverse kinematic, Denavit-Hartenberg (D-H) convention

**Abstract:** In this study, a gantry type welding robot having three prismatic and two rotational joints was used. By creating the kinematic diagram of this robot in Cartesian space its inverse kinematic equations were obtained. Denavit-Hartenberg rules defining the movement of one-link relative to another, were applied in drawing the kinematic diagram. The D-H method provides great easiness in forward and inverse kinematics calculations. With this method, the D-H parameters table to be used in kinematic calculations was created and inverse kinematic equations were obtained. Using inverse kinematic equations, the known position and orientation of the robot's end effector and the parameters of the position and orientation of each link were obtained. All these kinematic calculations were performed with a user interface software (GUI) prepared in Microsoft Visual Studio C# program. In this software, Mach3 program was also used as an assistant to control the motors with the position and orientation information obtained for each motor. In this way, a smooth welding application in the desired position and orientation is aimed.

## 5 DOF Gantry Tip Bir Kaynak Robotunun Ters Kinematik Hesaplamaları

### Anahtar Kelimeler

Homojen dönüşüm matrisi, Kinematik diyagram, Ters kinematik, Denavit-Hartenberg (D-H) yöntemi

**Öz:** Bu çalışmada, üç adet prizmatik ve iki adet döner ekleme sahip gantry tipi bir kaynak robotu kullanılmıştır. Bu robotun Kartezyen uzayında kinematik diyagramı oluşturularak ters kinematik denklemleri elde edilmiştir. Kinematik diyagramın çizilmesinde bir uzvun diğerine göre hareketini tanımlayan Denavit Hartenberg kuralları uygulanmıştır. D-H yöntemi, ileri ve ters kinematik hesaplamalarında oldukça kolaylık sağlamaktadır. Bu yöntem ile kinematik hesaplamalarda kullanılacak olan D-H parametreleri tablosu oluşturulmuş ve ters kinematik denklemler elde edilmiştir. Ters kinematik denklemler kullanılarak robotun uç efektörünün bilinen konum ve yönelimi ile her bir uzvun konum ve yönelimine ait parametreler elde edilmiştir. Tüm bu kinematik hesaplamalar Microsoft Visual Studio C# programında hazırlanan bir kullanıcı arayüz yazılımı (GUI) ile gerçekleştirildi. Bu yazılımda ayrıca her bir motora ait elde edilen konum ve yönelim bilgileri ile motorların kontrolünü yapabilmek için yardımcı olarak Mach3 programı kullanılmıştır. Bu sayede istenilen konum ve yönelimde düzgün bir kaynak uygulaması hedeflenmiştir.

### 1. INTRODUCTION

A robot is a multifunctional manipulator that can be created and programmed to perform a set of desired movements. According to ISO Standard 8373:1994, industrial robots should also have three or more joints. Robots are used in the manufacturing, transportation, etc.

of many products in the industry, provide many advantages in the processes in which they are used. These can be listed as speed, positioning accuracy, repeatability in operations, durability, safety, etc. Robots should be easily programmable in order to perform the operations given in production. Therefore, kinematic and dynamic

equations of the manipulator movements must be obtained [1-4].

The subfield of mechanics known as kinematics studies a mechanism's displacement, acceleration, and speed independent of the forces and moments forcing it to move [3].

The analytical study of manipulator movements is known as "robot kinematics". Kinematic modelling is very important for the analysis of the movements of the robot. In kinematic modelling, two space systems called three-dimensional Cartesian and four-dimensional Quaternion space are used [5]. Since the transformation data used in Cartesian Space is done using matrices or vectors, this model is called "point transformation". In Quaternion Space, linear vectors and quaternions are used to create the kinematic model, so this model is called "linear transformation method". Although Quaternion space provides ease of use in theoretical application with the use of complex numbers and is a method that provides faster results in computer environment, it is not preferred as much as Cartesian space in practice [6].

In Cartesian space geometry, five methods are generally used for kinematic modelling of the robot. These are the Homogeneous transformation method, Exponential method, SRK (Zero Reference Position) method, Pieper-Roth method, and TPS (Fully and Parametrically Continuous) method [6].

In the Cartesian coordinate, the transformation of robot arms relative to each other system is defined in two ways as rotation and translation. These transformations can be performed using the following methods: The definition of the Euler angle, calculation of the Gibbs vector, application of the Cayley-Klein parameters, Pauli spin matrices, orthonormal matrices, axis-angle, and Hamilton quaternions. In these expressions, homogeneous transformations based on 4x4 real matrices, called orthonormal matrices, are most widely used. In 1955, Denavit and Hartenberg found that the general transformation of the axes of two joints with respect to each other depends on four parameters. These parameters, called Denavit-Hartenberg (D-H) parameters, have been standardized to generate the kinematics of the robot [7]. Robot kinematics is analyzed in two parts as forward and inverse kinematics. Forward kinematics examines the relationships between the positions, velocities and accelerations of the robot links in space and the transformation matrices showing the relationship between the links are obtained. Inverse kinematics is the inverse of forward kinematics, where the link parameters are calculated based on the position and orientation values of the end-effector. Forward kinematics solutions are simple and straightforward. Therefore, we can say that the forward kinematic equation solutions of all manipulators can be obtained. On the other hand, inverse kinematic solutions of manipulators are a more difficult problem and solutions may not always be obtained. Inverse kinematics solutions for manipulators are primarily needed for calculating the torques of actuator joints and trajectory

planning. The relationship between forward and inverse kinematics is shown in Figure 1 [8].

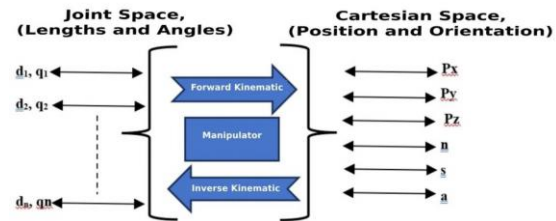


**Figure 1.** Schematic representation of the relationship between inverse kinematics and forward kinematics

There are many studies in the literature on forward and inverse kinematics:

Karakoyun et al. [1], in their study used the Bees Algorithm to determine the PID parameters for position control of a robot arm. In this study, mathematical modelling of the robot arm was performed with dynamic and kinematic calculations. Based on the simulations and calculations obtained, it was observed that the algorithms used to determine these parameters produced accurate results, and the robot's limb successfully reached the targeted reference point.

Altawile et al. [2], in their study realized a new methodology for the multitasking of a 2-wrist, 4-degree-of-freedom robotic arm to be used in agricultural applications. In this study, they used the Denavit-Hartenberg (D-H) method together with Lagrangian mechanics for kinetic and kinematic calculations of the robot.

Two different spaces, Cartesian and Quaternion, are used for kinematic modelling of robots. Some of the kinematic equation methods used in these models are suitable for forward kinematics, while others are useful for inverse kinematic solutions. When describing the same kinematic relation, the matrices obtained from the methods in Cartesian space contain more elements than the vector obtained in Quaternion space. Therefore, in a computer environment, the kinematic method described in Quaternion space works faster than the kinematic methods described in Cartesian space.

Kütük et al. [5], had used the Matlab programme to conduct forward and inverse kinematic analysis of a 6-axis DENSO robot with using a fully analytical solution. The Robotic Toolbox in Matlab® was included in studies of GUI (user interface) software, and simulation examples were obtained with this modelling. The outcomes were found to be identical when compared to analytical solutions.

Tonbul et al. [9], conducted inverse kinematic computations and trajectory planning of a five-axis Edubot robot with using the Matlab 5.02 program in their studies. They also observed changes in the robot's arms' joint angles, angular speeds, and angular accelerations

with time, and then applied the findings to the Edubot robot.

Kebria et al. [10], have simulated the mathematical kinematics and dynamics of a UR5 (universal robot) robot with 6 degrees of freedom by creating a position control system with a set of Matlab and Simmechanics models. Forward and inverse kinematics calculations were performed using DH parameters. The models are publicly available and can be easily used in Matlab environment.

Kaya et al. [11], created a D-H table according to the transformations of the lengths and axes of the robot arm produced from PLA material by additive manufacturing method in their study. According to this table, transformation matrices were found and forward and inverse kinematic calculations were obtained. In the study, image processing techniques and U2-Net artificial intelligence technique were used to detect objects and calculate their center of gravity.

Duran et al. [12], used the PID method to control the trajectory of a PUMA type robot arm with three degrees of freedom in their study. The joint parameters required for trajectory control using Cartesian coordinates were calculated using the inverse kinematics method. In this study, the system results obtained with three trajectory function inputs in the form of cycloid, harmonic and polynomial were compared in terms of proximity to the targeted trajectory.

Dikmenli [23], the kinematic analysis of robot was performed using analytical calculations in the study.

Filiposka et al. [24], developed a complete kinematic model for a 6-degree-of-freedom gantry-type CNC machine in their study. Using the Denavit-Hartenberg method, forward kinematic analysis was performed. The Jacobian matrix was utilized to examine singular configurations, and the reachable workspace was visualized in the Matlab environment. The presented parametric solutions were offered as a reference for both analysis of existing systems and the design of new machines.

In this study, the kinematic analysis of this robot was performed using analytical calculations. The kinematic diagram, frames and parameters of robot links were determined according to D-H rules and representation. Inverse kinematic equations were obtained with using D-H representation. All of these kinematic calculations were performed using a graphical user GUI developed in Microsoft Visual Studio C#. The welding operations have been applied correctly in the desired position and orientation.

## 2. MATERIAL AND METHOD

5 Degrees of Freedom (DOF) gantry-type welding robot was used, as shown in Figure 2. The robot has 3 prismatic and 2 rotary joints called as PPPRR notation. The robot's X, Y, and Z axes are supported by 1300 mm-long and 200 mm × 90 mm I-beam steel components.

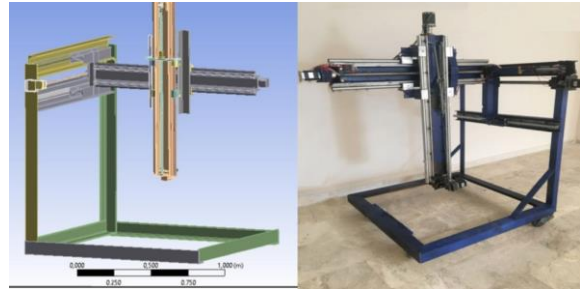


Figure 2. The welding robot's body

### 2.1. Robot Kinematic Modelling

The kinematic diagram of the robot was created in the Cartesian space. A schematic layout of the prismatic and rotational joints used in the robot was made to guide the robot end function from the base frame to the tool frame. One of the most common methods for constructing the kinematic diagram is D-H rules. Using the kinematic diagram, transformation matrices are obtained that give the transformation information of the joints with respect to each other (Figure 3).

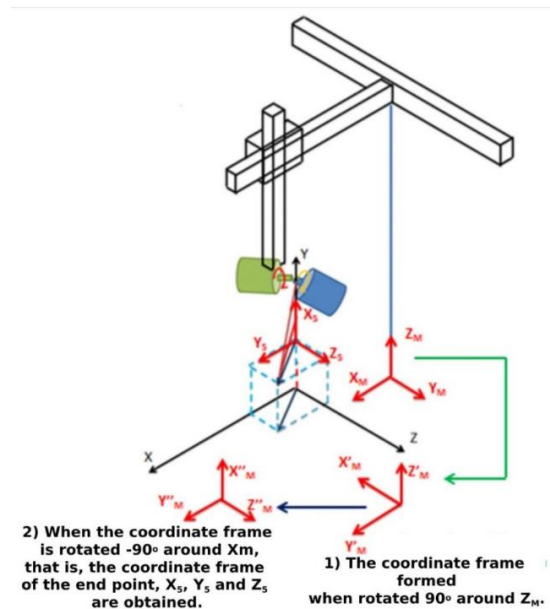


Figure 3. Rotational transformation based on axes

In 1955, Denavit and Hartenberg developed a standard for drawing kinematic diagrams of robotic applications with a set of rules.

While creating the kinematic diagram, the degree of freedom parameters was determined by considering the joint type as joint revolute and joint prismatic. The parameters for rotary joints were denoted by " $\theta$ " (angle) and for prismatic joints were denoted by " $d$ " (distance). In the kinematic diagram the joint offsets are indicated by " $d$ ", the link lengths are indicated by " $a$ " and the numbering of the links is done according to the joint number.

According to Denavit-Hartenberg rules, the joint axes are defined as following:

- The Z-axis is always aligned with the axis of the joint. If the joint is rotational, the Z-axis serves as the axis of rotation; for a prismatic joint, the Z-axis represents the axis along which the joint moves,
- The X-axis must be orthogonal to both the previous and current Z-axes and must intersect them,
- The Y-axis is determined using the right-hand rule, based on the assigned X and Z axes.

According to Denavit-Hartenberg rules, axes  $X_i, Y_i, Z_i$  all of joints of the robot were determined and a kinematic diagram was created as shown in Figure 4.

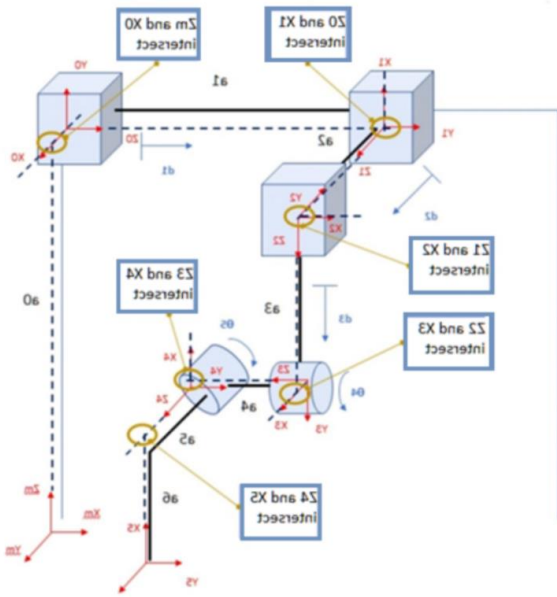


Figure 4. Determination of all axes and kinematic diagram according to D-H rules

The D-H convention is commonly used convention for obtaining frames in robotic applications. According to Denavit-Hartenberg convention, the link parameters are defined as following [16- 20]:

For  $i= 1...n$ ;

$\alpha_{i-1}$ =(link twist) the angle between  $Z_{i-1}$  and  $Z_i$  measured about  $X_{i-1}$ ;

$r_{i-1}$ =(link length) the distance between  $Z_{i-1}$  and  $Z_i$  measured along  $X_{i-1}$ ;

$d_i$ =( joint offset) the distance between  $X_{i-1}$  and  $X_i$  measured along  $Z_i$ ;

$\theta_i$ =(joint angle) the angle between  $X_{i-1}$  and  $X_i$  measured along  $Z_i$ ;

According to these D-H definitions, the parameters are obtained in Table1.

Table 1. Robot D-H parameters

$I$	$\theta_i$	$a_{i-1}$	$r_i$	$d_{i-1}$
1	90	90	0	$a_0$
2	90	90	0	$d_1+a_1$
3	90	-90	0	$d_2+a_2$
4	-90	90	0	$d_3+a_3$
5	$-90+\theta_4$	-90	0	$a_4$
6	$\theta_5$	0	$-a_6$	$a_5$

where  $a_0= 1m, a_1= 0.7m, a_2=0.7m, a_3 =0.7m, a_4= 0.1m, a_5= 0.1m$  and  $a_6= 0.3m$ .

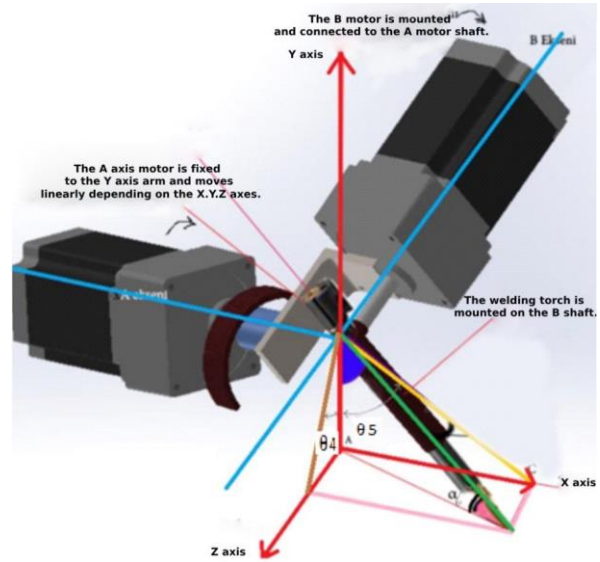


Figure 5. Perspective view of the robot's end-effector torch unit

In D-H convention, each homogeneous transformation matrices  $H_i$  is defined as multiplying four basic transformation matrices [21-26].

$$H = R_{z,\theta} Trans_{z,d} Trans_{x,a} R_{x,\alpha} \tag{1}$$

$$H_i^{i-1} = \begin{bmatrix} c_i & -s_i & 0 & 0 \\ s_i & c_i & 0 & 0 \\ 0 & 0 & 1 & 0 \\ 0 & 0 & 0 & 1 \end{bmatrix} \begin{bmatrix} 1 & 0 & 0 & 0 \\ 0 & 1 & 0 & 0 \\ 0 & 0 & 1 & d_{i-1} \\ 0 & 0 & 0 & 1 \end{bmatrix} \begin{bmatrix} 1 & 0 & 0 & r_i \\ 0 & 1 & 0 & 0 \\ 0 & 0 & 1 & 0 \\ 0 & 0 & 0 & 1 \end{bmatrix} \begin{bmatrix} 1 & 0 & 0 & 0 \\ 0 & c_j & -s_j & 0 \\ 0 & s_j & c_j & 0 \\ 0 & 0 & 0 & 1 \end{bmatrix} \tag{2}$$

The homogeneous transformation matrix for each joint is obtained as following (Equation 3.). Where  $c_i$  and  $s_i$  are shorthand for  $\cos\theta_i$  and  $\sin\theta_i$  and  $c_j$  and  $s_j$  are shorthand for  $\cos\alpha_i$  and  $\sin\alpha_i$  respectively.

$$H_i^{i-1} = \begin{bmatrix} \cos\theta_i & -\sin\theta_i \cos\alpha_i & \sin\theta_i \sin\alpha_i & r_i \cos\theta_i \\ \sin\theta_i & \cos\theta_i \cos\alpha_i & -\cos\theta_i \sin\alpha_i & r_i \sin\theta_i \\ 0 & \sin\alpha_i & \cos\alpha_i & d_{i-1} \\ 0 & 0 & 0 & 1 \end{bmatrix} \tag{3}$$

Equation 3. is homogeneous transformation matrix following by Equation 4. :

$$H_i^{i-1} = \begin{bmatrix} c_i & -s_i c_j & s_i s_j & r_i c_i \\ s_i & c_i c_j & -c_i s_j & r_i s_i \\ 0 & s_j & c_j & d_{i-1} \\ 0 & 0 & 0 & 1 \end{bmatrix} \tag{4}$$

The DH variables in Table 1 are substituted in Equation 4. to obtain the matrices in Equation 4.- Equation 8. :

$$H_0^M = \begin{bmatrix} 0 & 0 & 1 & 0 \\ 1 & 0 & 0 & 0 \\ 0 & 1 & 0 & a_0 \\ 0 & 0 & 0 & 1 \end{bmatrix} \quad (5)$$

$$H_1^0 = \begin{bmatrix} 0 & 0 & 1 & 0 \\ 1 & 0 & 0 & 0 \\ 0 & 1 & 0 & d_1 + a_1 \\ 0 & 0 & 0 & 1 \end{bmatrix} \quad (6)$$

$$H_2^1 = \begin{bmatrix} 0 & 0 & -1 & 0 \\ 1 & 0 & 0 & 0 \\ 0 & -1 & 0 & d_2 + a_2 \\ 0 & 0 & 0 & 1 \end{bmatrix} \quad (7)$$

$$H_3^2 = \begin{bmatrix} 0 & 0 & -1 & 0 \\ -1 & 0 & 0 & 0 \\ 0 & 1 & 0 & d_3 + a_3 \\ 0 & 0 & 0 & 1 \end{bmatrix} \quad (8)$$

$$H_4^3 = \begin{bmatrix} s_4 & 0 & c_4 & 0 \\ c_4 & 0 & s_4 & 0 \\ 0 & -1 & 0 & a_4 \\ 0 & 0 & 0 & 1 \end{bmatrix} \quad (9)$$

$$H_5^4 = \begin{bmatrix} c_5 & -s_5 & 0 & a_5 c_5 \\ s_5 & c_5 & 0 & a_5 s_5 \\ 0 & 0 & 1 & -a_6 \\ 0 & 0 & 0 & 1 \end{bmatrix} \quad (10)$$

The general homogeneous matrix used in forward kinematic calculations is determined. The general homogeneous matrix is obtained by multiplying the homogeneous matrices derived from the robot's base machine frame (denoted by "M") to the end-effector frame (5th frame) as shown in Equation 11. .

$$H_5^M = H_0^M H_1^0 H_2^1 H_3^2 H_4^3 H_5^4 = H_0^M H_2^1 H_3^2 H_4^3 H_5^4 \quad (11)$$

$$H_5^4 = \begin{bmatrix} s_5 & c_5 & 0 & a_1 - a_4 + d_1 + a_5 s_5 \\ s_4 c_5 & -s_4 s_5 & c_4 & a_2 - a_6 c_4 + d_2 + a_5 s_4 c_5 \\ -c_4 c_5 & c_4 s_5 & -s_4 & a_0 - a_3 - a_5 c_4 c_5 - d_3 + a_6 s_4 \\ 0 & 0 & 0 & 1 \end{bmatrix} \quad (12)$$

### 2.2. Inverse Kinematic

Inverse kinematic is the transformation process of position and orientation of robot end-effector tip from Cartesian space to joint space [2]. Also, determining joint parameters based on the end function's orientation (translation and rotational) data is known as inverse kinematics. Inverse kinematics solution is a commonly used and crucial technique for welding robot applications, handling robot applications, computing actuator joint torques, online control, trajectory planning, etc.

While forward kinematics is used to calculate the configuration of the robot's kinematic chain at the targeted location; inverse kinematics is used to obtain the parameters of the joints that generate these link movements. Inverse kinematics is used to derive the mathematical expression that computes the angular values for each link when the desired position and orientation are given.

$H_5^M = \begin{bmatrix} r_{11} & r_{12} & r_{13} & p_x \\ r_{21} & r_{22} & r_{23} & p_y \\ r_{31} & r_{32} & r_{33} & p_z \\ 0 & 0 & 0 & 1 \end{bmatrix}$  is the general homogeneous matrix

The machine link (Mth) inverse transformation matrix is premultiplied by each side of Equation 11. by using one of the matrix multiplication rules to find the identity matrix. It is given in Equation 13.;

$$(H_0^M)^{-1} * H_0^M = I \quad (13)$$

$$H_0^M * H_1^0 * H_2^1 * H_3^2 * H_4^3 * H_5^4 = H_5^M \quad (14)$$

Both sides of the Equation 14. is multiplied by  $(H_0^M)^{-1}$  and this expression turns into the following:

$$(H_0^M)^{-1} H_0^M H_1^0 H_2^1 H_3^2 H_4^3 H_5^4 = H_5^M (H_0^M)^{-1} \quad (15)$$

$$(H_0^M)^{-1} * H_5^M = \begin{bmatrix} r_{21} & r_{22} & r_{23} & P_y \\ r_{31} & r_{32} & r_{33} & P_z - a_0 \\ r_{11} & r_{12} & r_{13} & P_x \\ 0 & 0 & 0 & 1 \end{bmatrix} \quad (16)$$

$$(H_0^M)^{-1} * H_5^M = \begin{bmatrix} s_4 c_5 & -s_4 s_5 & c_4 & a_2 - a_6 c_4 + d_2 + a_5 s_4 c_5 \\ -c_4 c_5 & c_4 s_5 & -s_4 & -a_3 - a_5 c_4 c_5 - d_3 + a_6 s_4 \\ s_5 & c_5 & 0 & a_1 - a_4 + d_1 + a_5 s_5 \\ 0 & 0 & 0 & 1 \end{bmatrix} \quad (17)$$

The following equations are obtained from the known  $r_{ij}$  and  $P_x, P_y$  ve  $P_z$  robot end-effect coordinate values in Equation 16. And Equation 17. The two matrices calculated in these equations are equal to each other. The following equations are obtained by equating each  $(i, j)$  element of the matrices in these equations (Equation 16. and Equation 17.);

$$r_{11} = \sin\theta_5 \quad (18)$$

$$r_{12} = \cos\theta_5 \quad (19)$$

$$r_{13} = 0 \quad (20)$$

$$r_{21} = \sin\theta_4 \cos\theta_5 \quad (21)$$

$$r_{22} = -\sin\theta_4 \sin\theta_5 \quad (22)$$

$$r_{23} = \cos\theta_4 \quad (23)$$

$$r_{31} = -\cos\theta_4 \cos\theta_5 \quad (24)$$

$$r_{32} = \cos\theta_4 \sin\theta_5 \quad (25)$$

$$r_{33} = -\sin\theta_4 \quad (26)$$

$$P_x = a_1 - a_4 + d_1 + a_5 \sin\theta_5 \quad (27)$$

$$P_y = a_2 - a_6 \cos\theta_4 + d_2 + a_5 \sin\theta_4 \cos\theta_5 \quad (28)$$

$$P_z - a_0 = -a_3 - a_5 \cos\theta_4 \cos\theta_5 - d_3 + a_6 \sin\theta_4 \quad (29)$$

By dividing Equation 16. and Equation 17. ,  $\theta_5$  angle is found as following;

$$\tan \theta_5 = \frac{\sin \theta_5}{\cos \theta_5} = \frac{r_{11}}{r_{12}} \quad (30)$$

$$\theta_5 = \text{Atan2} \left( \frac{\sin \theta_5}{\cos \theta_5} \right) \quad (31)$$

By dividing Equation 21. and Equation 24.,  $\theta_4$  angle is found as following;

$$\tan \theta_4 = \frac{-\sin \theta_4}{\cos \theta_4} \quad (32)$$

$$\theta_4 = \text{Atan2} \left( \frac{\sin \theta_4}{\cos \theta_4} \right) \quad (33)$$

Using the known  $P_x$ ,  $a_1, a_4, a_5$  and  $\theta_5$  parameters the " $d_1$ " parameter is calculated from Equation 27. as following;

$$d_1 = P_x - a_1 + a_4 - a_5 \sin \theta_5 \quad (34)$$

Using the known  $P_y$ ,  $a_2, a_5, a_6, \theta_4$  and  $\theta_5$  parameters the " $d_2$ " parameter is calculated from Equation 28. as following;

$$d_2 = P_y - a_2 + a_6 \cos \theta_4 - a_5 \cos \theta_5 \sin \theta_4 \quad (35)$$

Using the known  $P_z$ ,  $a_0, a_3, a_4, a_5, a_6, \theta_5$  and  $\theta_4$  parameters the " $d_3$ " parameter is calculated from Equation 29. as following;

$$d_3 = -a_3 - a_5 \cos \theta_4 \cos \theta_5 + a_6 \sin \theta_4 - P_z + a_0 \quad (36)$$

The inverse kinematic equations for the 5-axis robot used in this study were provided above. Consequently, the inverse kinematic equations for the robot, whose end effector coordinates  $P_x, P_y$  ve  $P_z$  are known, were derived for the angle values  $\theta_4$  and  $\theta_5$  of the A and B rotational axes, as well as for the feed amounts  $d_1, d_2$  and  $d_3$ .

All these equations were carried out in a C# editor, and a user control GUI was developed. The developed GUI enabled the command of movement of the motors connected to the control unit at the desired rotational angles of  $\theta_4$  and  $\theta_5$ , as well as at the desired feed distances of  $d_1, d_2$  and  $d_3$  (Figure 6). The Mach3 program is added to GUI that is prepared in the Microsoft C# editor, as reference program. The obtained joint position parameters can be prepared in the form of a G-code text file using the GUI, as shown in Equation 37. .

$$N00 G01 X Y Z A (A) B (B) F 40 \quad (37)$$

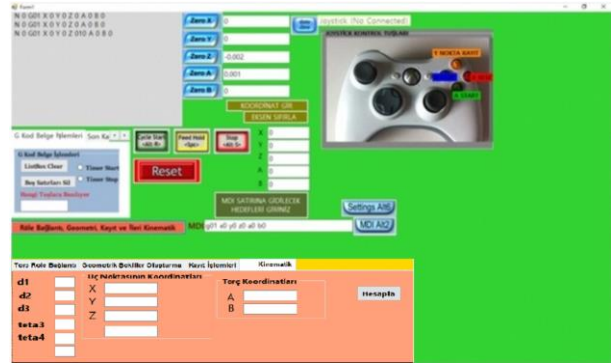


Figure 6. (GUI) User interface program

In the developed GUI, a trajectory text file was created to perform welding in the shape of the letter 'A'. For this welding application, the input data selected as the optimal welding parameters were a speed of 40 units/min, a 10 mm free wire length, and a 30° welding torch angle. These values were entered via the keyboard in the interface software, and the robot was instructed to perform the welding application (Figure 7).



Figure 7. Welding application for the letter "A"

Additionally, a G-code text file was created with the GUI for the word 'HARRAN' (Figure 8).

```
HARRAN BİTİŞİK - Not Defteri
Dosya Düzen Biçim Görünüm Yardım
| N 0 G01 X 0 Y 0 Z 0 A 0 B 0 F 1500
N 1 G01 X -2,49777530313971 Y -0,321794868166666 Z -0,277302585724274 A 1 B 0 F 1500
N 2 G01 X -4,99555060627943 Y -0,643589736333331 Z -0,554605171448549 A 2 B 0 F 1500
N 3 G01 X -7,49332590941914 Y -0,965384604499997 Z -0,831907757172823 A 3 B 0 F 1500
N 4 G01 X -9,99110121255886 Y -1,28717947266666 Z -1,1092103428971 A 4 B 0 F 1500
N 5 G01 X -12,4888765156986 Y -1,60897434083333 Z -1,38651292862137 A 5 B 0 F 1500
N 6 G01 X -14,9866518188383 Y -1,93076920899999 Z -1,66381551434565 A 6 B 0 F 1500
N 7 G01 X -16,984427121978 Y -2,25256407716666 Z -1,94111810006992 A 7 B 0 F 1500
N 8 G01 X -18,9822024251177 Y -2,57435894533332 Z -2,21842668579419 A 8 B 0 F 1500
N 9 G01 X -20,979977282574 Y -2,89615381349999 Z -2,49572327151847 A 9 B 0 F 1500
N 10 G01 X -22,9777530313971 Y -3,21794868166666 Z -2,77302585724274 A 10 B 0 F 1500
N 11 G01 X -24,9755283345369 Y -3,53974354983332 Z -3,05032844296702 A 11 B 0 F 1500
N 12 G01 X -26,9733036376766 Y -3,86153841799999 Z -3,32763182869129 A 12 B 0 F 1500
N 13 G01 X -28,9710789408163 Y -4,1833328616665 Z -3,60493361441557 A 13 B 0 F 1500
N 14 G01 X -30,968854243956 Y -4,50512815433332 Z -3,8822620813984 A 14 B 0 F 1500
N 15 G01 X -32,9666295470957 Y -4,82692302249998 Z -4,15953878586412 A 15 B 0 F 1500
N 16 G01 X -34,9644048502354 Y -5,1487178906665 Z -4,43684137158839 A 16 B 0 F 1500
N 17 G01 X -36,9621801533751 Y -5,47051275883331 Z -4,71414395731266 A 17 B 0 F 1500
N 18 G01 X -38,959954565149 Y -5,79230762699998 Z -4,99144654303694 A 18 B 0 F 1500
N 19 G01 X -40,9577307596546 Y -6,11410249516665 Z -5,26874912876121 A 19 B 0 F 1500
N 20 G01 X -42,9555060627943 Y -6,43589736333331 Z -5,54605171448549 A 20 B 0 F 1500
N 21 G01 X -44,9532813633333 Y -6,75769173633331 Z -5,82330258572427 A 21 B 0 F 1500
N 22 G01 X -46,951056627943 Y -7,0794868166666 Z -6,100605171448549 A 22 B 0 F 1500
N 23 G01 X -48,9488319303747 Y -7,4012815433332 Z -6,3779082302249998 A 23 B 0 F 1500
N 24 G01 X -50,9466072345369 Y -7,72307626999998 Z -6,65516381349999 A 24 B 0 F 1500
N 25 G01 X -52,9443825376766 Y -8,04487178906665 Z -6,93246654303694 A 25 B 0 F 1500
N 26 G01 X -54,9421578502354 Y -8,366677282574 Y -8,210249516665 Z -7,20977530313971 A 26 B 0 F 1500
N 27 G01 X -56,93993313971 Y -8,594453036376766 Y -8,4875307596546 Z -7,487051275883331 A 27 B 0 F 1500
N 28 G01 X -58,9377089408163 Y -8,8163328616665 Z -7,764230258572427 A 28 B 0 F 1500
N 29 G01 X -60,9354841799999 Y -9,09110121255886 Z -8,04153841799999 A 29 B 0 F 1500
N 30 G01 X -62,9332590941914 Y -9,36381551434565 Z -8,31882620813984 A 30 B 0 F 1500
N 31 G01 X -64,93103428971 Y -9,63651292862137 Z -8,59615381349999 A 31 B 0 F 1500
N 32 G01 X -66,928809408163 Y -9,9088765156986 Z -8,873466295470957 A 32 B 0 F 1500
N 33 G01 X -68,926584243956 Y -10,1811801533751 Z -9,15079486816666 A 33 B 0 F 1500
N 34 G01 X -70,924359408163 Y -10,45307626999998 Z -9,42810249516665 A 34 B 0 F 1500
N 35 G01 X -72,92213428971 Y -10,725363767666 Z -9,705415381349999 A 35 B 0 F 1500
N 36 G01 X -74,919909408163 Y -10,9977530313971 Z -9,98272327151847 A 36 B 0 F 1500
N 37 G01 X -76,917684604499997 Y -11,27007626999998 Z -10,260030258572427 A 37 B 0 F 1500
N 38 G01 X -78,9154604499997 Y -11,542379486816666 Z -10,537339572345369 A 38 B 0 F 1500
N 39 G01 X -80,9132354983332 Y -11,81464230258572427 A 39 B 0 F 1500
N 40 G01 X -82,91101021255886 Y -12,086945303694 Z -10,811633453694 A 40 B 0 F 1500
N 41 G01 X -84,90878502354 Y -12,3592487178906665 Z -11,0892506627943 A 41 B 0 F 1500
N 42 G01 X -86,90656027943 Y -12,631551434565 Z -11,36655381349999 A 42 B 0 F 1500
N 43 G01 X -88,9043354983332 Y -12,903854243956 Z -11,6438572327151847 A 43 B 0 F 1500
N 44 G01 X -90,9021103428971 Y -13,176157282574 Z -11,92116056627943 A 44 B 0 F 1500
N 45 G01 X -92,89988502354 Y -13,44845303694 Z -12,198463767666 A 45 B 0 F 1500
N 46 G01 X -94,8976604499997 Y -13,720766295470957 Z -12,47577089408163 A 46 B 0 F 1500
N 47 G01 X -96,8954354983332 Y -13,9930692302249998 Z -12,75307307596546 A 47 B 0 F 1500
N 48 G01 X -98,8932103428971 Y -14,265372327151847 Z -13,03037530313971 A 48 B 0 F 1500
N 49 G01 X -100,89098502354 Y -14,537677282574 Z -13,307677530313971 A 49 B 0 F 1500
N 50 G01 X -102,8887604499997 Y -14,809980762699998 Z -13,584980762699998 A 50 B 0 F 1500
N 51 G01 X -104,8865354983332 Y -15,08228302249998 Z -13,86228302249998 A 51 B 0 F 1500
N 52 G01 X -106,8843103428971 Y -15,35458572327151847 Z -14,13958572327151847 A 52 B 0 F 1500
N 53 G01 X -108,88208502354 Y -15,62688854243956 Z -14,41688854243956 A 53 B 0 F 1500
N 54 G01 X -110,8798604499997 Y -15,89919121255886 Z -14,69419121255886 A 54 B 0 F 1500
N 55 G01 X -112,8776354983332 Y -16,16649395731266 Z -14,97149395731266 A 55 B 0 F 1500
N 56 G01 X -114,8754103428971 Y -16,43879626999998 Z -15,24879626999998 A 56 B 0 F 1500
N 57 G01 X -116,87318502354 Y -16,7110990941914 Z -15,5260990941914 A 57 B 0 F 1500
N 58 G01 X -118,8709604499997 Y -16,98340178906665 Z -15,80340178906665 A 58 B 0 F 1500
N 59 G01 X -120,8687354983332 Y -17,2557045303694 Z -16,0807045303694 A 59 B 0 F 1500
N 60 G01 X -122,8665103428971 Y -17,5280072345369 Z -16,3580072345369 A 60 B 0 F 1500
N 61 G01 X -124,86428502354 Y -17,800310021255886 Z -16,635310021255886 A 61 B 0 F 1500
N 62 G01 X -126,8620604499997 Y -18,0726127151847 Z -16,9126127151847 A 62 B 0 F 1500
N 63 G01 X -128,8598354983332 Y -18,34491551434565 Z -17,18991551434565 A 63 B 0 F 1500
N 64 G01 X -130,8576103428971 Y -18,6172182574 Z -17,4672182574 A 64 B 0 F 1500
N 65 G01 X -132,85538502354 Y -18,8895210021255886 Z -17,7445210021255886 A 65 B 0 F 1500
N 66 G01 X -134,8531604499997 Y -19,161823767666 Z -18,021823767666 A 66 B 0 F 1500
N 67 G01 X -136,8509354983332 Y -19,4341265303694 Z -18,2991265303694 A 67 B 0 F 1500
N 68 G01 X -138,8487103428971 Y -19,7064292862137 Z -18,5764292862137 A 68 B 0 F 1500
N 69 G01 X -140,84648502354 Y -19,9787320313971 Z -18,8537320313971 A 69 B 0 F 1500
N 70 G01 X -142,8442604499997 Y -20,25103478906665 Z -19,13103478906665 A 70 B 0 F 1500
N 71 G01 X -144,8420354983332 Y -20,523337530313971 Z -19,408337530313971 A 71 B 0 F 1500
N 72 G01 X -146,8398103428971 Y -20,79564027943 Z -19,68564027943 A 72 B 0 F 1500
N 73 G01 X -148,83758502354 Y -21,06794302249998 Z -19,96294302249998 A 73 B 0 F 1500
N 74 G01 X -150,8353604499997 Y -21,34024577282574 Z -20,24024577282574 A 74 B 0 F 1500
N 75 G01 X -152,8331354983332 Y -21,6125485166665 Z -20,5175485166665 A 75 B 0 F 1500
N 76 G01 X -154,8309103428971 Y -21,8848513633331 Z -20,7948513633331 A 76 B 0 F 1500
N 77 G01 X -156,82868502354 Y -22,15715410249516665 Z -21,07215410249516665 A 77 B 0 F 1500
N 78 G01 X -158,8264604499997 Y -22,42945684604499997 Z -21,34945684604499997 A 78 B 0 F 1500
N 79 G01 X -160,8242354983332 Y -22,7017595854243956 Z -21,6267595854243956 A 79 B 0 F 1500
N 80 G01 X -162,8220103428971 Y -22,974062327151847 Z -21,904062327151847 A 80 B 0 F 1500
N 81 G01 X -164,81978502354 Y -23,246365072345369 Z -22,181365072345369 A 81 B 0 F 1500
N 82 G01 X -166,8175604499997 Y -23,51866777282574 Z -22,45866777282574 A 82 B 0 F 1500
N 83 G01 X -168,8153354983332 Y -23,790972530313971 Z -22,735972530313971 A 83 B 0 F 1500
N 84 G01 X -170,8131103428971 Y -24,06327527943 Z -23,01327527943 A 84 B 0 F 1500
N 85 G01 X -172,81088502354 Y -24,33557802249998 Z -23,29057802249998 A 85 B 0 F 1500
N 86 G01 X -174,8086604499997 Y -24,607880762699998 Z -23,567880762699998 A 86 B 0 F 1500
N 87 G01 X -176,8064354983332 Y -24,8801835166665 Z -23,8451835166665 A 87 B 0 F 1500
N 88 G01 X -178,8042103428971 Y -25,15248626999998 Z -24,12248626999998 A 88 B 0 F 1500
N 89 G01 X -180,80198502354 Y -25,4247890178906665 Z -24,4001789066665 A 89 B 0 F 1500
N 90 G01 X -182,7997604499997 Y -25,69709173633331 Z -24,67749173633331 A 90 B 0 F 1500
N 91 G01 X -184,7975354983332 Y -25,9693944854243956 Z -24,9547944854243956 A 91 B 0 F 1500
N 92 G01 X -186,7953103428971 Y -26,2416972327151847 Z -25,2320972327151847 A 92 B 0 F 1500
N 93 G01 X -188,79308502354 Y -26,5139999999999 Z -25,5093999999999 A 93 B 0 F 1500
N 94 G01 X -190,7908604499997 Y -26,7863027151847 Z -25,7867027151847 A 94 B 0 F 1500
N 95 G01 X -192,7886354983332 Y -27,0586054604499997 Z -26,0640054604499997 A 95 B 0 F 1500
N 96 G01 X -194,7864103428971 Y -27,33090820313971 Z -26,34130820313971 A 96 B 0 F 1500
N 97 G01 X -196,78418502354 Y -27,6032109572345369 Z -26,6186109572345369 A 97 B 0 F 1500
N 98 G01 X -198,7819604499997 Y -27,875513706376766 Z -26,895913706376766 A 98 B 0 F 1500
N 99 G01 X -200,7797354983332 Y -28,14781645303694 Z -27,17321645303694 A 99 B 0 F 1500
N 100 G01 X -202,7775103428971 Y -28,4201192021255886 Z -27,4505192021255886 A 100 B 0 F 1500
```

Figure 8. G code text document created with the interface program prepared in C# editor for the word "HARRAN"

### 3. RESULTS AND DISCUSSION

For this study, the proposed D-H convention was applied to draw the kinematic diagram. The D-H convention facilitates the calculation of forward and inverse kinematic calculations. The values of Table 1 given in Section 2.1 were obtained with this convention. Using the transformation matrices obtained with the help of the data in this table, the amounts of feed and rotation of each link required for inverse kinematic calculations were calculated both in the GUI and in Excel. In this way, the accuracy of the calculations with the use of these two programs was also proved. With these calculations, the amount of feeds ( $d_1, d_2$  and  $d_3$ ) and rotations ( $\theta_4$  and  $\theta_5$ ) required to be given to each motor that provides movement to the robot links at the coordinates where the end effector is desired to be found. According to the study, the solution results for 5 randomly selected test data are given in Table2.

**Table 2.** Solutions to the inverse kinematic problem

*Solution 1:*

$H^M_5 = \begin{vmatrix} 0.77 & 0.64 & 0.00 & 600.00 \\ 0.41 & -0.49 & 0.77 & 600.00 \\ 0.49 & -0.59 & -0.64 & 150.00 \\ 0.00 & 0.00 & 0.00 & 1.00 \end{vmatrix}$			
Inverse Kinematics Input Values (End Effector Position)		Inverse Kinematics Output Values	
$X$	600 mm	$d_1$	638 mm
$Y$	600 mm	$d_2$	82.3566 mm
$Z$	150 mm	$d_3$	743.24 mm
		$\theta_4$	40°
		$\theta_5$	50°

*Solution 2:*

$H^M_5 = \begin{vmatrix} 0.50 & 0.87 & 0.00 & 300.00 \\ 0.75 & -0.43 & 0.50 & 300.00 \\ 0.43 & -0.25 & -0.87 & 100.00 \\ 0.00 & 0.00 & 0.00 & 1.00 \end{vmatrix}$			
Inverse Kinematics Input Values (End Effector Position)		Inverse Kinematics Output Values	
$X$	300 mm	$d_1$	325.00 mm
$Y$	300 mm	$d_2$	-187.50 mm
$Z$	100 mm	$d_3$	785.05 mm
		$\theta_4$	60°
		$\theta_5$	30°

*Solution 3:*

$H^M_5 = \begin{vmatrix} 0.71 & 0.71 & 0.00 & 400.00 \\ 0.66 & -0.66 & 0.34 & 230.00 \\ 0.24 & -0.24 & -0.94 & 80.00 \\ 0.00 & 0.00 & 0.00 & 1.00 \end{vmatrix}$			
Inverse Kinematics Input Values (End Effector Position)		Inverse Kinematics Output Values	
$X$	400 mm	$d_1$	435.36 mm
$Y$	230 mm	$d_2$	-253.88 mm
$Z$	80 mm	$d_3$	810.92 mm
		$\theta_4$	20°
		$\theta_5$	45°

*Solution 4:*

$H^M_5 = \begin{vmatrix} 0.71 & 0.71 & 0.00 & 400.00 \\ 0.66 & -0.66 & 0.34 & 230.00 \\ 0.24 & -0.24 & -0.94 & 80.00 \\ 0.00 & 0.00 & 0.00 & 1.00 \end{vmatrix}$			
Inverse Kinematics Input Values (End Effector Position)		Inverse Kinematics Output Values	
$X$	280 mm	$d_1$	435mm
$Y$	110 mm	$d_2$	-264.381mm
$Z$	105 mm	$d_3$	809.021mm
		$\theta_4$	30°
		$\theta_5$	45°

*Solution 5:*

$H^M_5 = \begin{vmatrix} 0.77 & 0.64 & 0.00 & 400.0 \\ & & & 0 \\ 0.63 & -0.75 & 0.17 & 90.00 \\ 0.11 & -0.13 & -0.98 & 80.00 \\ 0.00 & 0.00 & 0.00 & 1.00 \end{vmatrix}$			
Inverse Kinematics Input Values (End Effector Position)		Inverse Kinematics Output Values	
$X$	400 mm	$d_1$	435mm
$Y$	90 mm	$d_2$	-404.381mm
$Z$	80 mm	$d_3$	809.021mm
		$\theta_4$	10°
		$\theta_5$	40°

In this study, kinematic calculations can be used with GUI to enable the robot to perform fully automatic welding with desired trajectory. The welding applications were successfully realized and the continuity of surface

welding was ensured. The developed Gantry welding robot provides a superior welding performance and it is seen that the GUI program is a user-friendly software.

#### 4. DISCUSSION AND CONCLUSION

In this study, a gantry type 5-DoF welding robot with three prismatic and two rotary joints is used. According to the reviews in the literature, the majority of industrial robots have 6 DOF degrees of freedom and have complex link structures. Therefore, analytical simplification of inverse kinematic solutions is difficult. Considering these limitations, an optimized welding robot has been designed especially for practical applications with high linear motion capability. For the motion analysis of this robot, a kinematic diagram in Cartesian space is constructed and inverse kinematic equations are obtained. D-H rules were applied to draw the kinematic diagram. The D-H method provides great convenience in forward and inverse kinematics calculations. The D-H parameters table to be used in kinematic calculations was created and inverse kinematic equations were obtained. Using the inverse kinematic equations, the known position and orientation of the end effector of the robot and the parameters of the position and orientation of each link were obtained. The analytical expressions obtained from the kinematic model calculation using the D-H convention were visually tested and checked with a user interface (GUI) in Microsoft C#. In this interface, user intervention is kept to a minimum and the superior capabilities of system automation are utilized by integrating Mach3 software. The use of G-code outputs used in CNC in Mach3 software provides an important convenience to the welding operator. In this way, welding applications were successfully realized and the continuity of surface welding was ensured.

The results obtained show that solvable systems are suitable for repeatable welding applications at industrial level. An effective position and orientation is provided in welding applications. Furthermore, the system can be quickly adapted to new positions with the use of GUI. The efficiency of this physical, kinematic model and the effectiveness of the software have been regularly verified. The flexible configuration of the system also supports various applications such as inspection, packaging and control. The 5-DoF robot is an important option for small-scale industries looking for automation solutions, both in terms of cost and usability. The system can be further developed to adapt complex applications such as image processing, AI-assisted healing or welding on non-linear surfaces. The design and manufacturing of the welding robot used in this study were carried out in the workshop of Harran University.

#### REFERENCES

- [1] Karakoyun, E., Çakan, A., & Kalyoncu, M. İki serbestlik dereceli bir robot kolun konum kontrolü için PID kontrol parametrelerinin arı algoritması (AA) kullanılarak belirlenmesi. *Balıkesir Üniversitesi Fen Bilimleri Enstitüsü Dergisi*. 2022;24(1): 111-124.
- [2] Altawil, B., & Can, F. C. Design and Analysis of a Four DoF Robotic Arm with Two Grippers Used in Agricultural Operations. *International Journal of Applied Mathematics Electronics and Computers*. 2023; 11(2): 79-87.
- [3] Sağlamer, E. Çoğul Robotlarda Hareket Koordinasyonunun Kuaternionlar ile Kinematik Olarak Modellenmesi ve Çözümü [Yüksek lisans Tezi]. İstanbul: İstanbul Teknik Üniversitesi Fen Bilimleri Enstitüsü; 2008.
- [4] Koç, S., & Şani, İ. Yapısal ve Kuvvet Analizi ile Doğrusal Tahrikli 3 Eksenli Endüstriyel Robotun Avantajlarının Belirlenmesi. *Avrupa Teknik Dergisi*. 2023; (EJT), 13(2): 174-183. <https://doi.org/10.36222/ejt.1230193>
- [5] Kütük, M. E., Daş, M. T., & Dülger, L. C. Forward and Inverse Kinematics Analysis of Denso Robot. In *Proceedings of The International Symposium of Mechanism and Machine Science*, 2017. Baku Azerbaijan: pp. 71-78.
- [6] Küçük, S., & Bingül, Z. Robot Sistemlerinde Kinematik Yöntemlerin Karşılaştırılması. *Politeknik Dergisi*. 2004; 7(2): 107-117.
- [7] Kucuk, S., ve Bingul, Z. Robot kinematics: Forward and Inverse Kinematics. *INTECH Open Access Publisher*. 2006; pp. 117-148).
- [8] Türker, K. S. Endüstride Kaynak Robotları (Proseslerin İncelenmesi ve Geliştirilmesi) [Yüksek lisans Tezi]. İstanbul: Gedik Üniversitesi Fen Bilimleri Enstitüsü; 2015.
- [9] Tonbul, T., & Sarıtaş, M. Beş Eksenli Bir Edobot Robot Kolunda Ters Kinematik Hesaplamalar ve Yörünge Planlaması. *Gazi Üniversitesi Mühendislik Mimarlık Fakültesi Dergisi*. 2013; 18(1).
- [10] Kebria, P. M., Al-Wais, S., Abdi, H., & Nahavandi. Kinematic and dynamic modelling of UR5 manipulator. In *2016 IEEE International Conference on Systems, Man, and Cybernetics (SMC)*, 2016. Budapest, Hungary: pp. 004229-004234.
- [11] Kaya, Z., Aksoy, B., & Özsoy, K. Eklemeli İmalat Yöntemiyle Üretilen Altı Eksenli Robot Kol ile Görüntü İşleme ve Yapay Zeka Tabanlı Ürünlerin Tasniflemesi. *Journal of Materials and Mechatronics*. 2023; A, 4(1): 193-210.
- [12] Duran, M. A., & Ankaralı, A. Üç serbestlik dereceli Puma tipi bir manipülâtörün PID kontrolü. *Selcuk University Journal of Engineering Sciences*. 2010; 9(1): 79-98. <https://sujes.selcuk.edu.tr/sujes/article/view/125/604>
- [13] Eberly, D. Euler Angle Formulas, *Geometric Tools*. Redmond WA 98052. USA:2020. <https://www.geometrictools.com/Documentation/EulerAngles.pdf>
- [14] De Luca . A. Robotics 1-Position and orientation of rigid bodies. *Sapienza University*. Rome: 2020. [https://homes.cs.washington.edu/~todorov/courses/cseP590/05\\_Kinematics.pdf](https://homes.cs.washington.edu/~todorov/courses/cseP590/05_Kinematics.pdf)
- [15] Bingül, Z. ve Küçük, S. *Robot Tekniği*. Birsen Yayınevi, İstanbul: 2005.
- [16] Abut, T., Soygüder, S., ve Alli, H. Bir Yıllansı Robotun Dinamik Analizi ve Kontrolü. 16. Ulusal Makina Teorisi Sempozyumu, Atatürk Üniversitesi,

2013. Erzurum.  
<http://dx.doi.org/10.13140/RG.2.1.1316.8080>
- [17] Garip, Z. Seri Robot Manipulatöründe Ters Kinematik Problemi Çözmek İçin Kaotik Tabanlı Çiçek Tozlaşma Algoritmasının Uygulanması. *Journal of the Institute of Science and Technology*. 2022; 12(1): 80-90.
- [18] Dereli, S., & Köker, R. 7-DOF Seri Robotun ters kinematik çözümünde eğitime amaçlı kullanılan çok katmanlı yapay sinir ağının tasarlanması ve sonuçların analizi. *Gaziosmanpaşa Bilimsel Araştırma Dergisi*. 2017; 6(1): 60-71.
- [19] Hocaoğlu, G. S., Çavli, N., & Benli, E. Altı Serbestlik Dereceli Robot Manipulatörün Ters Kinematik Analizi İçin Gko Ve Çdde Algoritmalarının Karşılaştırmalı Analizi. *Dokuz Eylül Üniversitesi Mühendislik Fakültesi Fen ve Mühendislik Dergisi*. 2024; 26(78): 449-457.
- [20] Ertugrul, S., Kaya, O., Turkmen, D., Eraslan, H., Taglioglu, G. B., & Gulec, M. O. Humanoid robot arm design, simulation, kinesthetic learning, impedance control and suggestions. *Journal of the Faculty of Engineering And Architecture of Gazi University*. 2022.
- [21] Duymazlar, O. 6 serbestlik dereceli seri robot kolunun ters kinematik analizi için hızlı algoritma geliştirilmesi ve uygulaması [Yüksek lisans Tezi]. İzmir: İzmir Üniversitesi Fen Bilimleri Enstitüsü; 2020.
- [22] Noreils, F. R. Inverse kinematics for a Humanoid Robot: a mix between closed form and geometric solutions. 2017; 1-31.
- [23] Dikmenli, S. Ofset ve küresel bilekli 6 serbestlik dereceli robotların ileri ve ters kinematik çözümü. *Avrasya Bilim Mühendislik ve Teknoloji Dergisi*. 2022; 3 (1): 14-28.
- [24] Filiposka, M., Djuric, A. M., & ElMaraghy, W. Kinematic analysis of a 6 dof gantry machine. 2015; SAE Technical Paper.